Transverse Instability of Bright Solitons in Hyperbolic dispersive Media

Simon-Pierre Gorza, Philippe Emplit, Marc Haelterman

OPERA-photonique, Université libre de Bruxelles CP 194/5; 50, Av. F.D. Roosevelt; B-1050 Bruxelles (Belgium)
Email: sgorza@ulb.ac.be

Thomas Trogdon, Bernard Deconinck

Department of Applied Mathematics, University of Washington, Campus Box 352420, Seattle, WA, 98195, USA

Abstract:
The theoretically predicted transition between snake and oscillatory snake instabilities of spatial bright solitons propagating in normally dispersive media is experimentally demonstrated. The oscillatory neck instability as a noncollinear four-wave-mixing process is also identified.

OCIS codes: (190.5530) Pulse propagation and solitons, (190.4420) Transverse effects in nonlinear optics.

Since the seminal work of Zakharov and Rubenchik on the stability properties of spatial solitons, it is well known that dispersion causes solitons to temporally break-up [1]. In normally dispersive media, the governing equation model is hyperbolic and the transverse instability of solitons manifests itself by a spatiotemporal zigzag shape deformation of the soliton beam, the so-called "snake instability". Following that work, it was commonly accepted that the soliton transverse instability band exhibits a finite cutoff (see Ref.[2] and references therein). Recently, it was however theoretically shown that only real growth rates are bounded and that there exist unstable modes of complex growth rates without cutoff, meaning that solitons are unstable against arbitrarily short wavelength perturbation [2]. In the same work, a new instability named "oscillatory" neck instability leading to the temporal oscillation of the soliton amplitude has also been identified.

In this work, we report on the experimental demonstration of both these new theoretical predictions for the instability of bright solitons propagating in normally dispersive media. We show that there is indeed no abrupt cutoff for high frequency perturbations but instead a slow decay of the instability gain, in agreement with theory. On the other hand, we experimentally demonstrate the oscillatory neck instability scenario and show that it results from a noncollinear four-wave-mixing process within the soliton beam.

In normally dispersive self-focusing planar waveguides, the slowly varying amplitude of an optical wave obeys the (2+1)D NLS equation. In dimensionless variables, this equation is written as

$$i\frac{\partial\psi}{\partial z} + \frac{1}{2}\frac{\partial^2\psi}{\partial x^2} - \frac{1}{2}\frac{\partial^2\psi}{\partial t^2} + |\psi|^2\psi = 0, \tag{1}$$

where z is the propagation coordinate, x is the transverse (in-plane) coordinate and t is the time.

We experimentally studied the stability of the spatial soliton solution of this equation, namely, $\psi = \mathrm{sech}(x)\exp(iz/2)$. To this end our experiments were performed with 4 mm-long semiconductor planar waveguides made up of $\mathrm{Al}_x\mathrm{Ga}_{1-x}\mathrm{As}$. The laser source is a picosecond mode-locked fiber laser generating 5 ps pulses at 1536 nm. Its output is split in two parts. The first part is sent into a low distortion Er-doped fiber amplifier to boost the peak power up to 3 kW. The output beam is then coupled into the waveguide to generate the spatial soliton. The second part is sent into a second fiber amplifier. Because of optical nonlinearities experienced in this amplifier, the output pulse spectrum is $\sim$ 200 nm-broad. A grating and lens arrangement is then used to shape a 10 nm-wide seed pulse which can be continuously tuned between 1480 nm and 1680 nm. The seed beam is then recombined and synchronized with the soliton beam before being coupled into the waveguide. A π-phase plate is inserted into the seed beam path when the snake instability has to be seeded. At the waveguide output, the beam is collected and sent to a two-dimensional spectrometer to record the angularly resolved spectrum.

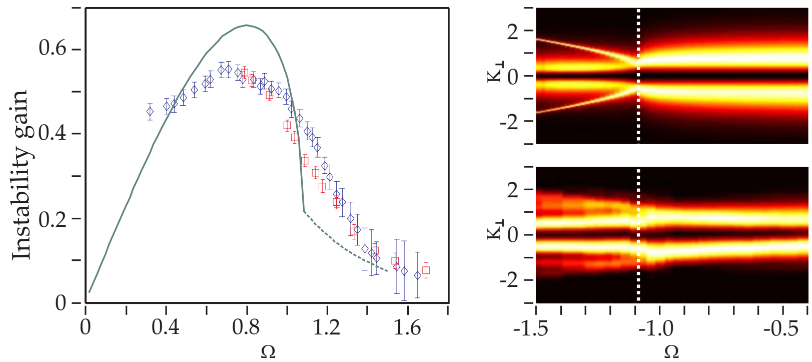

Fig. 1. Snake instability. Left: Theoretical gain for the snake (solid line) and the oscillatory snake (dashed line) instability. Experimental results with two different waveguides (squares and diamonds). Right: Sideband spatial spectrum as a function of the frequency detuning Ω. Top: angularly-resolved spectra computed from theory, bottom: experimental spectra recorded on the seed side. The white vertical dashed line separates the snake ($\Omega < 1.08$) from the oscillatory snake ($\Omega > 1.08$) regimes.

As can be seen in Fig.1, for small frequency detuning Ω, the snake instability gain starts to increase and reaches a maximum around $\Omega = 0.8$. Beyond this value, no abrupt cutoff is observed as expected from theory. Instead, the gain swiftly falls at first then for large Ω, a slower decrease is observed. At the same time, around the detuning $\Omega = 1.08$ the spatial spectrum of the frequency sidebands changes and is no longer a simple two-peaks structure as for smaller detuning. This is in very good agreement with theory and confirms that beyond this critical frequency detuning the snake instability is oscillatory. The theory indeed shows a qualitative difference between the unstable mode profiles of the snake instability and the oscillatory snake instability. This qualitative difference is clearly visible in our spectra. Note that deviations from theory can be readily explained by our experimental conditions since pulsed beams are used instead of continuous waves. Moreover, for large instability gain, higher harmonics are seen in the angularly resolved spectrum leading to a measured gain lower than the one expected from the linear perturbation analysis of Ref.[2].

Because of the hyperbolic nature of Eq.[1], solitons are robust against temporal periodic perturbations of their amplitude for small wavelength perturbations [1]. However, for $\Omega > 0.31$, solitons are subject to an oscillatory instability associated with complex gain [2]. The real part of this gain is lower than the snake instability gain but it can be investigated independently of the snake instability thanks to the use of a seed with symmetric spatial profiles. This unexpected instability can be explained by a noncollinear four-wave mixing process in which one of the two photons (f.i. at -Ω) is generated along the soliton beam axis while the second one (+Ω) is generated at an angle which depends on the frequency detuning. This is confirmed in the angularly-resolved spatial spectra of Fig.2.

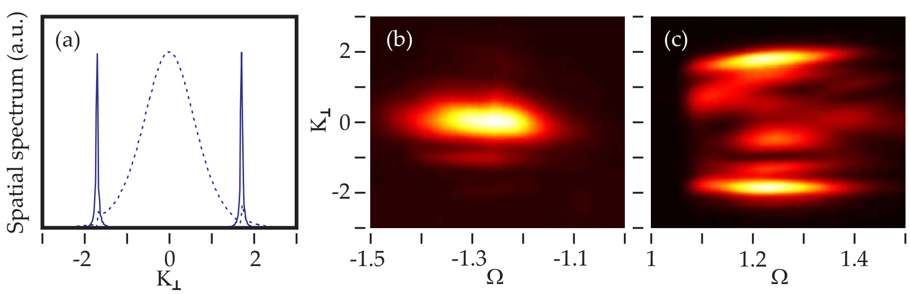

Fig. 2. Oscillatory neck instability. (a) Theoretical spatial spectra of the two sidebands: dashed (solid) line $\Omega = -1.22$ (+1.22). Experimental spatial spectra for a seed detuning of $\Omega = -1.22$: (b) signal, (c) idler.

In conclusion, our experiments allowed us to study the two new instability mechanisms predicted in Ref.[2]. In particular, we have demonstrated the transition between the snake instability and the oscillatory snake instability through the study of their gain spectra and the associated unstable mode profiles. The use of a spatially symmetric seed also allowed us to show evidence of the unexpected oscillatory neck instability as resulting from a noncollinear four-wave-mixing process.

[1] V. E. Zakharov and A. M. Rubenchik, "Instablity of waveguides and solitons in nonlinear media," Sov. Phys. JETP **38**, 494-500 (1974).

[2] B. Deconinck, *et al.*, "Transverse instabilities of deep-water solitary waves," Proc. Roy. Soc. A **462**, 2039-2061 (2005).